

1

2

3 Bursts of morphological and lineage diversification in modern
4 dasyurids, a “classic” adaptive radiation

5

6 VICENTE GARCÍA-NAVAS¹, MARTA RODRÍGUEZ-REY² AND MICHAEL WESTERMAN³

7

8 ¹ *Department of Integrative Ecology, Estación Biológica de Doñana (EBD-CSIC), Seville, Spain*

9 ² *Department of Biosciences, Swansea University, Swansea, Wales, United Kingdom*

10 ³ *Department of Ecology, Environment and Evolution, LaTrobe University, Melbourne,*

11 *Victoria, Australia*

12

13 Author for correspondence: Vicente García-Navas e-mail: vicente.garcianavas@gmail.com

14 *Department of Integrative Ecology, Estación Biológica de Doñana (EBD-CSIC), Américo*

15 *Vespucio 26, E-41092, Seville, Spain*

16

17

18 The Australasian marsupial family Dasyuridae exhibits one of the most spectacular species-
19 level diversity of any marsupial group. The existence of such exceptional species and
20 phenotypic diversity is commonly attributed to ecological opportunity (EO). According to the
21 EO hypothesis, organisms freed from the burden of competition may undergo an initial burst in
22 diversification and morphological evolution. Subsequently, as accessible niches become
23 occupied, rates of diversification should slow through time. We examined dynamics of lineage
24 and phenotypic diversification in order to test whether Dasyuridae diversified in a classic
25 adaptive radiation. We found that patterns of both lineage diversification and phenotypic (body
26 mass) disparity exhibited an early burst (EB) as predicted by the EO model. Three historical
27 events may have spurred this radiation: the extinction of thylacinids, the emergence of the New
28 Guinean cordillera, and the spread of arid habitats as evidenced by the existence of phylogenetic
29 clustering in these regions. In contrast to previous studies carried out in continent-wide systems,
30 our results support a niche-filling scenario with an EB signal strong enough to be detected. This
31 study shows that the Dasyuridae diversification fully conforms to the postulates of the EO
32 hypothesis and thus, it constitutes a “classic” adaptive radiation.

33

34 *Running head:* Diversification in dasyurid marsupials.

35 *Additional keywords:* Australia; evolutionary radiation; Dasyuridae; ecological opportunity;
36 macroevolution; marsupial.

37

INTRODUCTION

38

39 Australia and nearby islands have been exemplary subjects for studies of radiations of endemic
40 biota throughout the last century (see e.g., Mayr 1942). In fact, some Australian radiations -
41 mainly marsupials- inspired the seminal work of George G. Simpson, who coined the term
42 “ecological opportunity” to define an environment previously occupied by organisms for some
43 reason competitively inferior to its new inhabitants, and is nowadays considered one of the most
44 influential evolutionary biologists (Simpson 1944, 1953). Ecological opportunity is nowadays
45 defined as any event that could make niche space available, including emergence of new
46 environments, mass extinctions and key innovations that allows species to interact with the
47 environment in a novel way (i.e. new niche dimensions) (Stroud & Losos 2016). According to
48 the ecological opportunity (EO) hypothesis, the colonization of a novel or initially
49 underexploited adaptive zone is expected to lead to an early-burst of lineage diversification and
50 morphological evolution indicating that lineages are taking advantage of a niche space free of
51 competitors (Schluter 2000, Yoder *et al.* 2010). Subsequently, this is usually followed by a
52 density-dependent slowdown in the rate of speciation and phenotypic diversification as a result
53 of increased competition as ecological niches become filled (Seehausen 2006, Phillimore &
54 Price 2008, Rabosky & Lovette 2008). However, some authors have pointed out that this
55 pattern, the classic model of adaptive radiation, may be relatively uncommon in comparative
56 data (reviewed in Harmon *et al.* 2010; see also Venditti *et al.* 2011).

57 Although a relatively high proportion of studies of EO have been conducted in oceanic
58 islands (e.g., Caribbean Basin islands and Hawaiian archipelago; Gillespie 2004, Mahler *et al.*
59 2010) or islands *sensu lato* (mainland “lake” archipelagos; e.g., Wagner *et al.* 2012), during the
60 last five years the representation of continent-scale studies in the literature of adaptive radiations
61 has increased substantially (Bravo *et al.* 2014, Schweizer *et al.* 2014, Liedtke *et al.* 2016). Due
62 to their larger size, continents are in general more stable over time than islands and
63 consequently it has been suggested that the emergence of EO should be *a priori* less frequent in
64 mainland systems (Pinto *et al.* 2008). To date, evidence in favor of the EO hypothesis from
65 continental radiations is mixed. Some authors claim bursts of lineage and morphological
66 diversification, frequently linked to the colonization of an underexploited area (Schenk *et al.*

67 2013, Price *et al.* 2014), others have found a lack of signal attributable to the more complex
68 geographic and climatic histories of continents (Liedtke *et al.* 2016, Maestri *et al.* 2017).

69 Australia provides a very suitable scenario for studying diversification at a continental
70 scale. The progressive expansion of the Australian arid zone during the past 25 millions of years
71 appears to have spurred diversification in a number of plant and animal clades (reviewed in
72 Byrne *et al.* 2008). In fact, despite of its apparent topographic homogeneity, the Australian arid
73 region holds some of the most species-rich terrestrial vertebrate communities known including
74 that of sphenomorphine skinks (Rabosky *et al.* 2003), and the world's most diverse radiation of
75 subterranean diving beetles (Leys *et al.* 2003). In this regard, there is increasing evidence that
76 opportunities for speciation may have been great in this area (Crisp *et al.* 2004, Hugall *et al.*
77 2008, Catullo & Keogh 2014) suggesting a possible link between aridification and
78 diversification rates in several taxonomic groups. However, diversification rates have been
79 rigorously evaluated (for example, by means of lineage-through-time plots) in only a handful of
80 studies (see e.g., Rabosky *et al.* 2007), due to the fact that most of the data sets currently
81 available for arid-zone biota suffer from several drawbacks (mainly deficiencies in taxon
82 sampling and fossil calibration points), thus preventing the implementation of this type of
83 analyses (Byrne *et al.* 2008).

84 Dasyuridae is a family of marsupials comprising two subfamilies (Dasyurinae,
85 Sminthopsinae) and four tribes (Dasyurini, Phascogalini, Sminthopsini and Planigalini). It
86 constitutes the principal radiation of insecto-carnivorous mammals within Australasia. Of the 75
87 described species, 52 are restricted to Australia and 14 to New Guinea and surrounding islands;
88 two species are present on both sides of Torres Strait. Many dasyurids are small (7-30 g) and
89 mouse-like but the group also contains the larger cat-sized quolls (*Dasyurus* spp., up to 7 kg.),
90 as well as the Tasmanian devil (*Sarcophilus harrisii*), which at ~10 kg represent the largest
91 extant species. Dasyurids are found in habitats ranging from montane rainforests to nearly
92 rainless deserts of inland Australia, and most of biogeographic associations (i.e., Eremaean
93 species, Torresian species, etc.) are represented within the four tribes, a feature characteristic of
94 Australo-Papuan radiations (e.g., Christidis *et al.* 2011). The existence of this striking within-
95 clade disparity in terms of biogeography suggests that the colonization of arid environments

96 from mesic habitats did not occur in one wave (i.e., multiple independent evolution)
97 (Westerman *et al.* 2016).

98 In this study, we used a time-calibrated phylogeny, data on body mass and community
99 phylogenetics to test for macro-evolutionary patterns predicted by the EO hypothesis in modern
100 dasyurids. According to the EO model, organisms freed from the burden of competition, such as
101 through the colonization of a novel or underexploited environment, should experience an
102 ecological “release” characterized by increased cladogenesis (early phase) followed by a
103 progressive slowdown in diversification rate (late phase) (Schluter 2000, Harmon *et al.* 2010).
104 We tested for the existence of this temporal pattern in this iconic marsupial radiation. Regarding
105 phenotypic diversification, predictions of EO are fundamentally expected to apply to traits that
106 are correlated with ecological niches (Schluter 2000). Therefore, we tested whether
107 morphological disparity is partitioned among rather than within subclades using one
108 morphological trait that is strongly associated with niche: body mass (Fisher *et al.* 2011). Body
109 mass is a key trait in dasyurids as well as in other mammals, as it influences fitness through its
110 effects on reproduction (larger males have priority access to females; Kraaijeveld-Smit *et al.*
111 2003, Fisher & Cockburn 2006) and survival (Körtner & Geiser 2009). If the radiation of a
112 lineage has been adaptive, it is expected that the diversification dynamics of both the lineage
113 and the phenotype show signal of diversity-dependent diversification (niche-filling) over time.
114 Thus, both diversity dimensions should exhibit similar patterns (Schluter 2000). In addition, we
115 tested for a relationship between body mass and the two main environmental variables,
116 temperature and precipitation, which vary markedly across the distribution range of this group.
117 The existence of a phenotype-environment correlation is one of the four criteria that have been
118 suggested to be necessary for adaptive radiations to take place (Schluter 2000). The three
119 remaining are: common ancestry, trait utility (experimental or theoretical tests of performance
120 or fitness of a trait in its corresponding environment) and rapid bursts of speciation. The two
121 phylogenetic criteria, *viz.* common ancestry and rapid speciation, are examined using the
122 molecular data (see above). Finally, we tested for the existence of phylogenetic structure
123 (underdispersion or “clustering”), which might be indicative of *in situ* diversification.
124 Specifically, the presence of phylogenetic clustering in environments different from the zone

125 colonized by the most recent common ancestor has been previously interpreted as evidence for
126 the existence of a burst in diversification rate upon entering a new area (Cardillo 2011).

127

128

129

MATERIAL AND METHODS

130 *Data set*

131 Our study comprised 68 out of extant 75 dasyurid species (i.e., 91% of extant species). The
132 following seven species were excluded from the present study since these were not included in
133 the phylogenetic study (Westerman *et al.* 2016, see more below) in which this study is based on:
134 *Phascolosorex doriae*, *Sminthopsis boullangerensis* (a species of dunnart found only on
135 Boullanger Island and formerly considered a subspecies of *S. griseoventer*), *A. adustus*, *A.*
136 *subtropicus*, *A. mysticus*, *A. argentus* and *Antechinus arktos*. The last five species belong to the
137 Australian dusky Antechinus complex and some of them have been recently described (*A.*
138 *mysticus*: Baker *et al.* 2012; *A. argentus*: Baker *et al.* 2013; *A. arktos*: Baker *et al.* 2014).

139 The fossil record for this family includes *Barinya wangala* (Wroe 2003), the currently
140 oldest recognized dasyurid dating back from the middle Miocene and which has been placed in
141 its own subfamily, Barinyainae. The remaining putative extinct dasyurids have never been
142 described and their placement within Dasyuridae remains unclear and controversial
143 (summarized in Black *et al.* 2012).

144

145 *Phylogeny and divergence time estimates*

146 Analyses conducted here are based on the phylogenetic estimate and associated divergence
147 times presented in a recent study (Westerman *et al.* 2016). In this study, Westerman and
148 colleagues reassessed the phylogenetic relationships of 68 of 75 living dasyurids species using a
149 large molecular database comprising published and novel sequences for eight nuclear genes
150 [*breast cancer early onset gene 1 (BRCA1)*, *apolipoprotein B gene (ApoB)*, *recombination*
151 *activating gene 1 (RAG1)*, *von Willibrand Factor gene (vWF)*, *embryonic globin gene intron 1*
152 (*ε-globin*), *protamine P1 (protP1)*, *interphotoreceptor binding protein (IRBP)* and *beta*
153 *fibrinogen intron (bfib7)*] and seven mitochondrial genes [*cytb*, *12S rRNA*, *tRNA valine plus 16S*

154 *rRNA, nicotinamide dehydrogenase (NADH) genes 1 and 2, and cytochrome oxidase genes (COI*
155 *and COII)]* to yield a total DNA sequence database of over 17 kb. Divergence time estimates
156 were performed using BEAST v.1.8 (Drummond *et al.* 2006) with the uncorrelated lognormal
157 relaxed molecular clock (see Westerman *et al.* 2016 for more details). Our present analyses
158 were performed using the maximum clade credibility (MCC) tree provided in that study. In
159 addition, we used a set of 1 000 trees randomly sampled from the posterior distribution of the
160 Markov chain Monte Carlo (MCMC) search in order to account for phylogenetic uncertainty.

161

162 *Morphological and ecological data*

163 We compiled data on average adult body mass (g) from the literature (both primary sources and
164 summary publications; e.g., Van Dyck *et al.* 2013) for each species. Body mass and body length
165 (size) are strongly correlated ($r^2 = 0.96, p < 0.001$). We obtained similar results when using body
166 length as focal trait and thus, for the sake of brevity, we only report results for body mass. Body
167 mass was log-transformed prior to analyses.

168

169 *Diversification analyses*

170 To visualize the pattern of diversification we constructed a lineage-through-time (LTT) plot,
171 which illustrates the deviation of the empirical LTT pattern from the expectation under a
172 constant-rate pure-birth process (Harmon *et al.* 2003). For the empirical LTT plot, we calculated
173 the 95% confidence interval (CI) from our sample of trees (1 000 trees). We determined the
174 extent to which branching events in our phylogeny depart from those expected under a constant-
175 rate process by computing the gamma (γ) statistic (Pybus & Harvey 2000) in the R package
176 *laser* (Rabosky 2006). A deceleration in diversification rate is inferred when $\gamma \leq -1.645$, which
177 is interpreted as evidence for the existence of an early-burst of diversification (Harmon *et al.*
178 2003). We assessed γ by using the Monte Carlo constant-rate (MCCR) test, as this approach
179 allows accounting for incomplete sampling. We performed these analyses on the MCC tree as
180 well as on our set of 1 000 trees randomly sampled from the posterior distribution of the
181 Markov chain Monte Carlo (MCMC) search in order to account for phylogenetic uncertainty.
182 To further test for temporal slowdowns in diversification rate consistent with adaptive radiation,

183 we applied a model-fitting strategy in *laser*. We compared the fit of two-constant rate models (1
184 and 2) and three variable -rate models (3-5): (1) a pure-birth (PB) or Yule model; (2) a birth-
185 death (BD) model; (3) an exponential diversity-dependent (DDX) model, which models the
186 speciation rate as a function of the number of extant lineages at any time point and may be
187 increasing or decreasing; (4) a logistic diversity-dependent (DDL) speciation rate model, in
188 which the number of lineages increases until reaching a k limit analogous to the ‘carrying
189 capacity’ parameter of population ecology, and (5) a BD variable-rate model with the speciation
190 rate r_1 shifting to r_2 at a time t (yule-2-rate). Model-fit was compared using the bias-corrected
191 version of the Akaike Information Criterion (AICc). In order to test for constancy of
192 diversification rates, we computed the $\Delta\text{AIC}_{\text{RC}}$ statistics: $\text{AIC}_{\text{RC}} = \text{AIC}_{\text{H0}} - \text{AIC}_{\text{H1}}$, where AIC_{H0} is
193 the AIC score of the best rate-constant model and AIC_{H1} is the AIC score of the best rate-
194 variable model. This model comparison was performed using the function “fitdAICrc” in *laser*.
195 When $\Delta\text{AIC}_{\text{RC}} > 0$, then the best of the rate-variable models is also the best model for the
196 observed diversification pattern; when $\Delta\text{AIC}_{\text{RC}} < 0$, the best rate-constant model would be
197 favored (Rabosky & Lovette 2008).

198 In addition, we examined changes in rates of diversification across the MCC tree by
199 means of Bayesian Analysis of Macroevolutionary Mixtures (BAMM v.2.5; Rabosky *et al.*
200 2014). This approach uses reversible-jump Markov chain Monte Carlo (rjMCMC) to fit models
201 with one or more diversification regimes to subsets of the tree. We ran four chains of 100 000
202 000 generations each, sampled every 50 000 generations. The first 10 000 000 generations were
203 discarded as burn-in. We set starting parameters priors with the setBAMMpriors function in the
204 R package *BAMMtools* (Rabosky *et al.* 2017). We identified a credible set of distinct shift
205 configurations that account for 95% of the probability of the data.

206

207 *Morphological disparification*

208 First, we tested for phylogenetic signal in body mass using Blomberg’s K statistic (Blomberg *et al.*
209 *al.* 2003) as implemented in the R package *phytools* (Revell 2012). Values of K near 1 indicate a
210 strong phylogenetic signal, whereas values near 0 denote a decoupling of phylogenetic and
211 phenotypic divergence. K values > 1 indicate that some factor is causing closely related species

212 to be more ecologically similar than would be expected under random walk (i.e. niche
213 retention).

214 Subsequently, we tested the EO prediction of an early-burst in morphological trait
215 divergence, leading to proportionately greater disparity than expected under a BM model early
216 in group' evolutionary history, and a lower proportion of phenotypic variation partitioned within
217 subclades by means of disparity-through-time (DTT) plots (Harmon *et al.* 2003). DTT plots
218 illustrate relative subclade disparity, that is, mean squared pairwise Euclidean distances between
219 all species in morphospace in each subclade whose ancestral lineages were present at that time,
220 relative to the disparity of the entire taxon (Harmon *et al.* 2003). In order to quantify such a
221 difference, we computed the morphological disparity index (MDI), which represents the sum of
222 the areas between the curve describing the average disparity of the trait and the curve describing
223 the expected disparity under a null model of BM (1 000 simulated datasets). A negative MDI
224 score would indicate that early subclade disparity was lower (and among subclade disparity
225 higher) than expected under BM, which is consistent with that predicted by the EO model
226 (Harmon *et al.* 2003). We carried out DTT analysis for body mass and size using the *geiger*
227 package (Harmon *et al.* 2008).

228 We also tested the EO prediction of a decline in the rate of phenotypic evolution
229 through time by means of two complementary methods: by using the node height test
230 (Freckleton & Harvey 2006), and by using a model-based approach that assessed which models
231 of trait evolution provides a better fit to our data. First, we calculated phylogenetic independent
232 contrasts (PICs) for each morphological trait and correlated the absolute value of the PIC to the
233 height of the nodes from which they were generated. A negative correlation is predicted when
234 evolution follows a niche-filling model, because as niches become filled with increasing species
235 number the differences among the niches of ancestors and descendants become progressively
236 smaller (Freckleton & Harvey 2006). Secondly, we quantified the tempo and mode of trait
237 diversification by fitting three alternative models that describe different evolutionary patterns:
238 (i) the Brownian motion model (BM, which describes a random walk of trait evolution along
239 branches in the phylogeny), (ii) the early-burst or "niche-filling" model (EB, where rates
240 exponentially decrease over time under the assumption that niches are saturated by

241 accumulating species within lineages), and (iii) the Ornstein-Uhlenbeck model (OU, which
242 assumes that selection pulls the trait values around an adaptive optimum, i.e. “bounded”
243 evolution). Models were run using *geiger* and their goodness-of-fit were compared using AICc
244 and AIC weights (AICw). In addition, we tested for increasing or decreasing evolutionary rates
245 using Pagel’s delta, δ . When $\delta > 1$ it implies that evolutionary change is concentrated towards
246 the tips (i.e., accelerated trait rates) and $\delta < 1$ towards the root (i.e. slowed trait rates). In a
247 further step, we tested for trait-dependent diversification related to body mass in the dasyurids
248 using BAMM. According to the EB model, trait evolution slows at the same pace across the
249 entire clade (Slater & Pennell 2014). We tested for congruence between rates of lineage and
250 phenotypic diversification resulting from EO (Price *et al.* 2016).

251 Lastly, we tested for the existence of a relationship between body mass and two
252 environmental variables: mean annual temperature and annual precipitation. We extracted mean
253 annual temperature and mean annual precipitation layers (*BIO1* and *BIO12*, respectively) from
254 WorldClim database (Hijmans *et al.* 2005) for a 100×100 km resolution grid in which we
255 calculated the average value of both abiotic variables for each grid cell using QGIS (QGIS
256 Development Team 2016). Thereby, we obtained mean values of temperature and precipitation
257 for each dasyurid species. We then examined associations between phenotype (body mass) and
258 environmental factors (temperature, precipitation) independent of similarity due to phylogeny
259 by means of Phylogenetic Generalized Least Squares (PGLS) implemented in the *caper* package
260 (Orme *et al.* 2012).

261

262 *Phylogenetic species clustering*

263 We employed a community phylogenetics approach (Kembel 2009) to depict the phylogenetic
264 structure of species assemblages. A pattern of phylogenetic clustering might indicate in-situ
265 speciation whereas a pattern of phylogenetic over-dispersion might indicate either extensive
266 regional competitive exclusion or multiple allopatric speciation (Cardillo 2011, Mazel *et al.*
267 2016). To that end, we divided the observed geographic ranges into seven biogeographic
268 regions based on Fox & Archer 1984: (1) Eremaean region, (2) south-western temperate (SW),
269 (3) non-tropical east (NTE) or Bassian region, (4) monsoon or Torresian region, (5) Irian region

270 (remnant rainforests), (6) New Guinea, and (7) Tasmania. Dasyurid species were coded as
271 present (=1) or absent (=0) in each region (species were allowed to occur in multiple regions)
272 based on distribution data available from the International Union for Conservation of Nature
273 (the IUCN Red List of Threatened Species; www.iucnredlist.org) that were checked against
274 distribution maps provided in the Atlas of Living Australia (www.ala.org.au) and Global
275 Biodiversity Information Facility (GBIF, www.gbif.org). For each biogeographic region, we
276 calculated mean pairwise distance (MPD) and mean nearest taxon distance (MNTD) (Webb *et*
277 *al.* 2002) using the R package *picante* (Kembel *et al.* 2010). MPD and MNTD increase with
278 phylogenetic evenness (larger phylogenetic distances among species of an assemblage) and
279 decreases with clustering (shorter phylogenetic distances). MPD is a measure of the average
280 branch length distance among all species pairs in a given community and thus, it is thought to be
281 more sensitive to phylogeny-wide patterns of phylogenetic clustering and over-dispersion.
282 Meanwhile, MNTD is the branch length distance between each species and its closest relative in
283 a community and thus, this measure is more sensitive to patterns of clustering and over-
284 dispersion closer to the tips of the tree. Standardized effect size (*z*-value) was computed for both
285 metrics by shuffling tip labels 999 times to generate a null distribution for each metric and
286 comparing the observed value to the null distribution under a “independentswap” model. We
287 obtained very similar results when considering alternative null models (results not shown).
288 Differences in patterns of clustering and overdispersion at shallow (MNTD) and deeper (MPD)
289 levels in the phylogeny might indicate support for a niche-filling scenario (Cardillo 2011, Lv *et*
290 *al.* 2016).

291

292

293

RESULTS

294 *Diversification*

295 The LTT analysis for Dasyuridae revealed a decline in diversification toward the present (Fig.
296 1a). Around 16-17 Ma diversification rates tend to decrease through time and most modern
297 dasyurid genera and species already existed before the latest Miocene. The obtained gamma
298 statistic ($\gamma_{MCC} = -6.445$, $p < 0.001$) indicated that the internal nodes are closer to the root than

309 expected under the pure-birth model (i.e. early rapid diversification), rejecting the null
300 hypothesis of a constant-rate of cladogenesis over time. When the constant-rate test was
301 performed on the set of 1000 chronograms, we obtained a rather similar γ value ($\gamma_{1000} = -5.568$).
302 The one-tailed test yielded a statistically significant result in 90.9% (909/1000) of cases.
303 Consistent with the LTT analysis, results of the birth-death likelihood analysis indicate that
304 DDL (logistic-density dependent model) was the best-fitting model in both cases (Table 1),
305 which suggests that Dasyuridae diversification has tended to decline over time as a function of
306 accumulating species. The DDL model provided a better fit than the preferred rate-constant
307 (PB) model ($\Delta AIC_{rc} = 45.86$). Yet, the yule-2-rate model also received substantial support from
308 the data (Table 1).

309 The BAMM analyses detected no rate shift; none of the branches were associated with a
310 speciation-extinction rate slowdown.

311

312 *Morphological disparity*

313 We found a significant phylogenetic signal for body mass ($K = 1.44$, $p = 0.001$). The obtained K
314 value indicates that longer branches (old lineages) contribute proportionally more to trait
315 evolution, which supports the EB model (Hernández *et al.* 2013). Relative disparity of body
316 mass was lower than expected under Brownian motion (Fig. 1b), but this departure was non-
317 significant ($p = 0.117$). The negative MDI value (MDI = -0.225) indicates that disparity tends to
318 be distributed among subclades. Consistent with the EO hypothesis, we found a significant
319 negative relationship between node height and contrast values, which indicates that the rate of
320 body mass evolution decreased as the number of species increased (estimate: -0.055 ± 0.023 , $t =$
321 -2.36 , d.f. = 65, $p = 0.02$; Fig. 1c). Maximum likelihood model fitting results for body mass
322 indicate that the EB model was the best model ($\Delta AIC_c > 4$; Table 2). Mean values for r , the
323 parameter from the EB model that describes the rate at which trait evolution slows through time,
324 were moderately high ($r_{MCC} = -0.115$; $r_{1000} = -0.111$) in comparison with the r estimates
325 provided in [10] ($r = -0.007$, range: -0.15 to 0). Accordingly, the obtained delta value ($\delta =$
326 0.273) indicates that the rates of body mass evolution have slowed over time.

327 We further investigated the temporal rate dynamics and rate heterogeneity of body mass
328 evolution using BAMM. Five distinct configurations emerged after we identified a 95% credible
329 set of distinct shift configurations: no shifts (posterior probability [PP] = 0.50) and one shift-
330 located in the Dasyurus clade- for the remaining four configurations (PP = 0.26, 0.13, 0.04 and
331 0.03; see Supporting Information). Thus, in congruence with the pattern of lineage
332 diversification, there was no evidence overall for a rate shift in body mass evolution.

333 When exploring the existence of a phenotype-environment correlation, we found a
334 significant negative association between body mass and mean annual temperature (PGLS; $F_{1,66}$
335 = 7.65, $p < 0.007$; Fig. 3). The relationship between body mass and annual precipitation was not
336 significant ($p > 0.5$).

337

338 *Phylogenetic species clustering*

339 We found a significant pattern of phylogenetic clustering irrespective of the employed measure
340 (MPD or MNTD) for the assemblage of species inhabiting New Guinea (Table 3). According to
341 the obtained MPD values, the Eremaean assemblage also shows a significant pattern of
342 underdispersion across the whole phylogeny (Table 2). On the contrary, both the NTE and
343 Torresian region have small MNTD values because, within these regions, each species has a
344 close relative in the assemblage, but the MPD values does not differ significantly from the null
345 model because the distance matrix contains both very large and very small distances (see Fig. 2)
346 and the average of these is almost equal to the overall average edge length (Table 3). We
347 obtained almost identical results when combining NTE and Tasmania, and the Australian
348 rainforests (Irian region) and New Guinea into two single categories (see Supporting
349 Information).

350

351

DISCUSSION

352 The ecological theory of adaptive radiation predicts accelerated rates of speciation associated
353 with divergence in ecologically relevant phenotypic traits like body size/mass (e.g. Schluter
354 2000, Losos 2010). This phenomenon may arise if a trait changes more rapidly in some species

355 than others in response to selective pressures. This change may facilitate rapid access to
356 underexploited ecological niches or increased reproductive isolation, thereby boosting the
357 speciation rate. Our results provide compelling evidence for the existence of congruent bursts of
358 lineage and morphological diversification in the dasyurid radiation, meeting thus the predicted
359 pattern of adaptive diversification shaped by ecological opportunity (EO).

360

361 *Lineage diversification in modern dasyurids*

362 According to the EO model, organisms freed from the burden of competition, such as through
363 the invasion of a novel or underexploited habitat, should experience a “release” characterized by
364 increased cladogenesis (accelerated speciation rates and decreased extinction rates) and
365 associated phenotypic diversification. Subsequently, clades should show a slowdown in
366 speciation toward the present as niche space became saturated (Schluter 2000). Our results
367 support this hypothesis; we found that the model that predicts a density-dependent decline in
368 diversification rates (DDL model) provided the best approximation to the observed pattern of
369 lineage accumulation through time. This result suggests that the tempo of dasyurid
370 diversification may be mediated by ecological interactions among relatives. Limited ecological
371 opportunity emerging from increased intraspecific competition and shortage of available
372 ecological niches may explain the existence of diversity-dependent diversification in this
373 radiation (Rabosky & Lovette 2008, Phillimore & Price 2008). Although this pattern of reduced
374 speciation rates following a burst in diversity has also been detected in studies at continental
375 scale (Burbrink & Pyron 2009), most evidence comes from studies carried out in geographically
376 confined regions (lakes: Seehausen 2006, Wagner *et al.* 2012, islands: Harmon *et al.* 2003),
377 where once niches are filled, diversification rate can only decline. By contrast, in vast
378 continental regions, organisms may encounter new ecological opportunities successively, and
379 the colonization of these underexploited zones may suppose the maintenance of a constant-rate
380 of diversification (Derryberry *et al.* 2011). Regarding this, it should be noted that although
381 Australia is considered by definition a continent, its reduced size in comparison with other
382 landmasses (e.g. Eurasia, Africa, North America) and its climatic characteristics (predominance

383 of arid and semi-arid regions) make it a kind of “big island”, which may explain that Australian
384 radiations are more similar to those found in islands than to other continental ones.

385 In agreement with that predicted by the density-dependent model, our findings suggest
386 that this evolutionary radiation has existed long enough for the net diversification rate to plateau
387 (Weir 2006, Rabosky & Lovette 2008, Rabosky 2013). Alternatively the slowdown in
388 diversification could be explained with the simple assumption that speciation takes time rather
389 than occurs instantaneously (protracted speciation). That is, speciation events that initiated in
390 the recent past may not have completed yet, so they do not count towards the total number of
391 extant species at the present (Etienne & Rosindell 2012, Moen & Morlon 2014). Frequent
392 peripatric speciation could also lead to diversification slowdowns without niche differentiation
393 (Pigot *et al.* 2010). Under this model, one species with a wide geographic range gives rise to
394 many small-ranged species that are unlikely to further speciate, leading to a linear increase in
395 species over time (“geography of diversification”; Moen & Morlon 2014). This hypothesis is
396 plausible since closely related species of dasyurids rarely show range overlap. Thus, the role of
397 geography in explaining diversification slowdowns deserves to be explored in further studies.
398 On the other hand, although the DDL model provided the best fit to our data, the yule-2-rate
399 also received substantial support suggesting the possible existence of a sudden change in the
400 rate of diversification. That abrupt shift could have been occurred about 16 millions of years
401 ago, once niches become filled (see Fig. 1a).

402

403 *Morphological disparity: strong support for the EB model*

404 To the best of our knowledge, ours is the first study providing evidence for the existence of an
405 EB pattern across an entire family using the three main approaches for detecting early bursts of
406 trait evolution in comparative datasets: disparity-through-time (DTT) analysis (Harmon *et al.*
407 2003), the node height test (Freckleton & Harvey 2006), and maximum-likelihood (ML)
408 (Harmon *et al.* 2010). Of these three methods, the most conservative and less frequently
409 employed is ML. For example, Harmon and colleagues (2010) carried out an extensive analysis
410 on a large number of comparative datasets (including some clades that are traditionally
411 considered textbook examples of adaptive radiation like Galápagos finches or *Anolis* lizards)

412 and they found that only one out of the forty-nine clades analyzed supported the EB model
413 using ML, concluding that it may be due to either the absence of “classic” adaptive radiations or
414 the ephemerality of the EB signal. Regarding this latter, Slater & Pennell (2014) argued that the
415 EB model has received little support in the literature as it cannot be easily detected with
416 phylogenetic comparative data rather to the absence of this pattern in nature. In fact, a few
417 authors have found support for decelerating rates of evolution in certain clades (Burbrink &
418 Pyron 2009, Derryberry *et al.* 2011) but, interestingly, none of these studies employed a ML
419 approach to do so. Our results are certainly striking as they provide evidence that early bursts of
420 phenotypic evolution are completely identifiable in moderately sized phylogenies (50-100 taxa)
421 using ML model fitting when a series of circumstances are met. Regarding this, it is worth
422 mentioning that although Cooper & Purvis (2010) reported that the inferred rate of body mass
423 (not size) evolution in the Tasmanian devil was exceptionally high (see also Venditti *et al.*
424 2011), our results remained similar when excluding this comparatively large species from our
425 data set (i.e. strong support for the EB model; Akaike weights, EB: 0.96, OU: 0.01, BM: 0.03).
426 Thus, the detected burst is not attributable to an explosive increase confined to one branch
427 (Tasmanian devil). In other words, our results are not driven by a single unusual datum.

428

429 *Phenotype-environment correlation*

430 By definition, adaptive radiations generally involve phenotypic diversification along one or
431 more ecological dimensions of specialization (Schluter 2000, Yader *et al.* 2010). The existence
432 of a phenotype-environment correlation is one of the four criteria employed by Schluter (2000)
433 to define a radiation as adaptive. Here, we have shown that the dasyurid radiation seems to meet
434 that criterion. We found a negative correlation between body mass and annual temperature,
435 suggesting that dasyurid species may have reduced their body size to adapt to warmer
436 environments (Rodríguez *et al.* 2006, Gohli & Voje 2016). The higher surface area-to-volume
437 ratio of smaller animals (e.g. dunnarts) in hot and dry climates facilitates body heat loss through
438 the skin and thus, helps cool the body (e.g. Brown & Lee 1969). Furthermore, body mass has
439 been shown to be associated with daily torpor, a strategy to reduce energy expenditure during
440 the winter period (Geiser & Baudinette 1990). As daily torpor lowers daily energy and water

441 requirements, it may be crucial for survival and reproduction of dasyurid species in the arid
442 zone (Holloway & Geiser 1996, Körtner & Geiser 2009). Thus, a lower body mass may
443 consistently confer fitness benefits, which is in agreement with the Schluter' third criterion: trait
444 utility. Yet, experimental tests are necessary to confirm this hypothesis. In addition, the
445 existence of adaptive diversification in relation to habitat use is also certainly plausible in the
446 radiation of Dasyuridae according to the observed ecological disparity: some species are entirely
447 terrestrial (e.g. *Sminthopsis* spp.), other species are semi-arboreal (e.g. *Antechinus stuartii*, *A.*
448 *bellus*) and some others (e.g. *Murexia longicaudata*, *Phascogale tapoatafa*) are arboreal
449 specialists. Thus, adaptation to distinctive structural habitats may explain the remarkable
450 phenotypic differences that can be found among dasyurid species. For example, semi- or
451 arboreal species like the spotted-tailed quoll *Dasyurus maculatus* have a well-developed hallux
452 and limb ratios indicative of a slow-running and an arboreal life-style. This toe tends to be
453 reduced or absent in more terrestrial species like the eastern quoll *D. viverrinus*, which is
454 adapted to the open grasslands and exhibits a low femur/metatarsal ratio indicating faster
455 running speeds (Jones & Stoddart 1998). Habitat partitioning (both vertical and horizontal)
456 would reduce competition for food among sympatric species as it has been shown in dasyurid
457 communities (Jones 1997). This suggests that competition, both intra- and interfamily (see
458 above), seems to be an important force behind this adaptive radiation and it has influenced size
459 relationships among species. In fact, character displacement has been demonstrated for this
460 guild (Jones & Barmute 2000), which constitutes evidence of competition operating on an
461 evolutionary time scale. Further studies using morphological measurements (e.g. limb size, tail
462 length) from museum specimens would provide insight into the association between phenotype
463 and habitat use, and other ecomorphological relationships in this family.

464

465 *Phylogenetic species clustering*

466 The arid zone (Eremaean region) showed “basal” clustering as expected taking into account that
467 basal lineages in each of the dasyurid tribes are comprised of arid taxa -reflecting that the rise of
468 modern dasyurids is linked to the colonization of more xeric-arid environments- and that MPD
469 is more strongly influenced by the basal structure of the phylogenetic tree. This pattern suggests

470 that arid lineages underwent a rapid niche-filling radiation, with rates of diversification slowing
471 in more recent times as expected under density-dependent models of speciation (see also
472 Cardillo 2011). In the NTE and Torresian region, MNTD values suggested phylogenetic
473 structuring which were not evident from MPD values. This pattern of “terminal” clustering
474 reflects a relatively high proportion of sympatric congeners in disparate clades, which might be
475 promoted by niche partitioning via fine-scale habitat preferences. The MNTD measures solely
476 the nearest phylogenetic neighbor for each species and thus, it seems to be a better index of
477 potential competition in a given assemblage (Mazel *et al.* 2016). The New Guinean assemblage
478 showed both “basal” and “terminal” clustering probably due to its more recent origin. Our
479 results suggest that the niche-filling process (rapid radiation and subsequent slowdown)
480 occurred primarily in the arid region, which has been frequently regarded as biodiversity engine
481 (“species pump”; Byrne *et al.* 2008). In fact, the arid region harbors a higher diversity (24
482 species) than any other region (Fig. 2). This finding is in agreement with previous studies
483 showing rapid diversification in Australian arid environments (Rabosky *et al.* 2007, Powney *et*
484 *al.* 2010). The greatest species richness observed in the Eremaean region, as opposed to the zone
485 from which dasyurids originated (sclerophyll and woodlands habitats; Krajewski *et al.* 2000a),
486 suggests the existence of a burst in diversification rate upon colonizing this previously
487 unexploited environment (Schweizer *et al.* 2014, Lv *et al.* 2016).

488

489 *Major features of an exceptional radiation*

490 So, what makes this radiation special? Why does the radiation of dasyurid marsupials retain the
491 EB signal in both lineage and trait data? Probably, the most important feature is the elevated
492 synchronicity of this radiation. The four tribes exhibit major cladogenic events from the early to
493 middle Miocene (23-15 Ma) and before the end of this epoch most modern dasyurid genera and
494 species, including those from New Guinea, were already in existence (Westerman *et al.* 2016,
495 Krajewski *et al.* 2000a). Most splits in each of the four dasyurid subfamilies appear to coincide
496 with two historical episodes: the spread of more open woodland-grassland habitats during the
497 early-mid Miocene and the waves of dispersal into proto-New Guinean islands (Black *et al.*
498 2012). On the other hand, the rise of modern dasyurids has often been claimed to be associated

499 with the climate-driven extinction of archaic thylacinids and bandicoots, which dominated the
500 insectivorous-carnivorous niche during the late Oligocene to middle Miocene and whose
501 ecological role was occupied by the smaller dasyurids during the latter half of the Neogene
502 (Krajewski *et al.* 2000b, Wroe 2003). Hence, a relaxation of interspecific competition (due to
503 the progressive decline in thylacinid diversity) in conjunction with the availability of new
504 underexploited areas appears to underlie this rapid and explosive radiation. It is likely that these
505 factors led to an EB signal too strong to be eroded by later processes.

506

507 *Conclusions*

508 In this study we provide one of the clearest examples of “classic” adaptive radiation described
509 so far for a mammal group. In fact, the Dasyuridae fulfills at least three of the four criteria for
510 adaptive radiation (*sensu* Schluter 2000). Both diversification and morphological disparity
511 analyses provided strong evidence for the role of EO as the main stimulus for the emergence of
512 exceptionally diverse clades (Glor 2010, Losos 2010, Stroud & Losos 2016). Our results show
513 that both lineage diversification and body size disparity showed the same pattern of slowdown
514 toward the recent. Such a congruent pattern -the core prediction from adaptive radiation theory-
515 is hardly ever found, especially in analyses without the fossil record (Slater & Pennell 2014,
516 Slater 2015a,b). The existence of phylogenetic clustering in several regions supports the idea of
517 a multiple explosive radiation of species as main characteristic of the diversification process in
518 this family. This study constitutes an exception to the common assumption that constant-rate
519 lineage and trait diversification is the most pervasive model in continent-scale radiations (Tran
520 2014, Alhajeri *et al.* 2016, Liedtke *et al.* 2016). Overall, our findings indicate that some
521 radiations in nature resemble perfectly a niche-filling scenario as predicted by the EO theory.

522

523 **Acknowledgements**

524 Matthew Pennell and Mauro Sugawara an anonymous referee commented an earlier draft of this
525 manuscript. V.G.N was supported by a “Juan de la Cierva” fellowship from Spanish Ministry of
526 Economy and Competitiveness (FPDI-2013-16828). M.R.R was supported by a PhD fellowship

527 funded by Aquainvad-ED, a Marie Skłodowska-Curie Innovative Training Network (H2020-
528 MSCA-ITN-2014-ETN-642197).

529

530

531

REFERENCES

532 Alhajeri, B.H., Schenk, J.J. and Steppan, S.J. 2016. Ecomorphological diversification following
533 continental colonization in muroid rodents (Rodentia: Muroidea). *Biol. J. Linn. Soc.*, 117, 463-
534 481.

535 Baker, A.M., Mutton, T.Y. and Van Dyck, S. 2012. A new dasyurid marsupial from eastern
536 Queensland, Australia: the Bufffooted Antechinus, *Antechinus mysticus* sp. nov. (Marsupialia:
537 Dasyuridae). *Zootaxa*, 3515, 1-37.

538 Baker, A.M., Mutton, T.Y. and Hines, H.B. 2013. A new dasyurid marsupial from Kroombit
539 Tops, south-east Queensland, Australia: the Silver-headed Antechinus, *Antechinus argentus* sp.
540 nov. (Marsupialia: Dasyuridae). *Zootaxa*, 3746, 201-239.

541 Baker, A.M., Mutton, T.Y., Hines, H.B. and Van Dyck, S. 2014. The Black-tailed Antechinus,
542 *Antechinus arktos* sp. nov.: a new species of carnivorous marsupial from montane regions of the
543 Tweed Volcano caldera, eastern Australia. *Zootaxa*, 3765, 100-133.

544 Black, K.H., Archer, M., Hand, S.J. and Godthelp, H. 2012. *The rise of Australian marsupials:
545 a synopsis of biostratigraphic, phylogenetic, palaeologic and palaeobiogeographic
546 understanding*. In: Talent, J.A., (ed.) *Earth and life: global biodiversity, extinction intervals and
547 biogeographic perturbations through time*. New York, Springer, 983-1078.

548 Blomberg, S.P., Garland, T. and Ives, A.R. 2003. Testing for phylogenetic signal in comparative
549 data: behavioral traits are more labile. *Evolution*, 57, 717-745.

550 Bravo, G.A., Remsen Jr. J.V. and Brumfield, R.T. 2014. Adaptive processes drive
551 ecomorphological convergent evolution in antwrens (Thamnophilidae). *Evolution*, 68, 2757-
552 2774.

553 Burbrink, F.T. and Pyron, R.A. 2009. How does ecological opportunity influence rates of
554 speciation, extinction, and morphological diversification in new world ratsnakes (tribe
555 Lampropeltini)? *Evolution*, 64, 934-943.

556 Brown, J.H. and Lee, A.K. 1969. Bergmann's Rule and Climatic Adaptation in Woodrats
557 (*Neotoma*). *Evolution*, 23, 329-338.

558 Byrne, M., Yeates, D.K., Joseph, L., Kearney, M., Bowler, J., Williams, M.A.J., Cooper, S.,
559 Donnellan, S.C., Keogh, J.S., Leys, R. & Melville, J., Murphy, D.J., Pouch, N. and Wyrwoll, K.-

560 H. 2008. Birth of a biome: insights into the assembly and maintenance of the Australian arid
561 zone biota. *Mol. Ecol.*, 17, 4398-4417.

562 Cardillo, M. 2011. Phylogenetic structure of mammal assemblages at large geographical scales:
563 linking phylogenetic community ecology with macroecology. *Phil. Trans. R. Soc. B*, 366, 2545-
564 2553.

565 Catullo, R.A. and Keogh, J.S. 2014. Aridification drove repeated episodes of diversification
566 between Australian biomes: Evidence from a multi-locus phylogeny of Australian toad lets
567 (*Uperoleia*: *Myobatrachidae*). *Mol. Phyl. Evol.*, 79, 106-117.

568 Christidis, L., Irestedt, M., Rowe, D., Boles, W.E. and Norman, J.A. 2011. Mitochondrial and
569 nuclear DNA phylogenies reveal a complex evolutionary history in the Australasian robins
570 (*Passeriformes*: *Petroicidae*). *Mol. Phyl. Evol.* 71, 726-738.

571 Cooper, N. and Purvis, A. 2010. Body size evolution in Mammals: complexity in tempo and
572 mode. *Am Nat.* 175, 727-738.

573 Crisp, M., Cook, L. and Steane, D. 2004. Radiation of the Australian flora: what can
574 comparisons of molecular phylogenies across multiple taxa tell us about the evolution of
575 diversity in present-day communities? *Phil. Trans. R. Soc. Lond. B: Biol. Sci.*, 359, 1551-1571.

576 Derryberry, E.P., Claramunt, S., Derryberry, G., Chesser, R.T., Cracraft, J., Aleixo, A., Pérez-
577 Emán, J., Renssen Jr, J.V. and Brumfield, R.T. 2011. Lineage diversification and morphological
578 evolution in a large-scale continental radiation: the neotropical ovenbirds and woodcreepers
579 (*Aves*: *Furnariidae*). *Evolution*, 65, 2973-2986.

580 Drummond, A.J., Ho, S.Y.W., Phillips, M.J. and Rambaut, A. 2006. Relaxed phylogenetics and
581 dating with confidence. *PLoS Biology*, 4, e88.

582 Etienne, R.S. and Rosindell, J. 2012. Prolonging the past counteracts the pull of the present:
583 protracted speciation can explain observed slowdowns in diversification. *Syst. Biol.*, 61,
584 204-213.

585 Fisher, J.T., Anholt, B. and Volpe, J.P. 2011. Body mass explains characteristic scales of habitat
586 selection in terrestrial mammals. *Ecol. Evol.* 1, 517-528.

587 Fox, B. and Archer, E. 1984. The diet of *Sminthopsis murina* and *Antechinus stuartii* in
588 sympatry. *Aust. Wildl. Res.*, 11, 235-248.

589 Freckleton, R.P. and Harvey, P.H. 2006. Detecting non-Brownian trait evolution in adaptive
590 radiations. *PLoS Biol.*, 4, e373.

591 Geiser, F. and Baudinette, A. 1990. The relationship between body mass and rate of rewarming
592 from hibernation and daily torpor in mammals. *J. Exp. Biol.*, 151, 349-359.

593 Gillespie, R. 2004. Community assembly through adaptive radiation in Hawaiian spiders.
594 Science, 303, 356-59.

595 Glor, R.E. 2010. Phylogenetic insights on adaptive radiation. Ann. Rev. Ecol. Evol. Syst., 41,
596 251-270.

597 Harmon, L. J., Schulte II, J.A., Larson, A. and Losos, J.B. 2003. Tempo and mode of
598 evolutionary radiation in Iguanian lizards. Science, 301, 961-964.

599 Harmon, L.J., Weir, J.T., Brock, C.D., Glor, R.E., and Challenger, W. 2008. GEIGER:
600 investigating evolutionary radiations. Bioinformatics, 24, 129-131.

601 Harmon L.J., Losos J.B., Jonathan Davies T., Gillespie R.G., Gittleman J.L., Bryan Jennings
602 W., Kozak K.H., McPeck M.A., Moreno-Roark F., Near T.J., Purvis A., Ricklefs R.E., Schluter
603 D., Schulte II, J.A., Seehausen O., Sidlauskas B.L., Torres-Carvajal O., Weir J.T. and Mooers
604 A.O. 2010. Early bursts of body size and shape evolution are rare in comparative data.
605 Evolution, 64, 2385-2396.

606 Hernández, C.E., Rodríguez-Serrano, E., Avaria-Llautureo, J., Inostroza-Michael, O., Morales-
607 Palleró, B., Boric-Bargetto, D., Canales-Aguirre, C.B., Marquet, P.A. and Meade, A. 2013.
608 Using phylogenetic information and the comparative method to evaluate hypotheses in
609 macroecology. Methods Ecol. Evol., 4, 401-415.

610 Holloway, J.C. & Geiser, F. 1996. Reproductive status and torpor of the marsupial *Sminthopsis*
611 *crassicaudata*: effects of photoperiod. J. Therm. Biol. 21, 373-380.

612 Hugall, A.F., Foster, R., Hutchinson, M. and Lee, M.S.Y. 2008. Phylogeny of Australasian
613 agamid lizards based on nuclear and mitochondrial genes: implications for morphological
614 evolution and biogeography. Biol. J. Linn. Soc., 93, 343-358.

615 Jones, M.E. 1997. Character displacement in Australian dasyurid carnivores: size relationships
616 and prey size patterns. Ecology, 78, 2569-2587.

617 Jones, M.E. and Stoddart, D.M. 1998. Reconstruction of the predatory behavior of the extinct
618 marsupial thylacine (*Thylacinus cynocephalus*). J. Zool., 246, 239-246.

619 Jones, M.E. and Barmute, L.A. 2000. Niche differentiation among sympatric Australian
620 dasyurid carnivores. J. Mammal., 81, 434-447.

621 Kembel, S.W., Cowan, P.D., Helmus, M.R., Cornwell, W.K., Morlon, H., Ackerly, D.D.,
622 Blomberg, S.P. and Webb, C.O. 2010. *Picante*: R tools for integrating phylogenies and ecology.
623 Bioinform., 26, 1463-1464.

624 Kembel, S.W. 2009. Disentangling niche and neutral influences on community assembly:
625 assessing the performance of community phylogenetic structure tests. Ecol. Lett., 12, 949-960.

626 Kraaijeveld-Smit, F.J.L., Ward, S.J. and Temple-Smith, P.D. 2003. Paternity success and the
627 direction of sexual selection in a field population of a semelparous marsupial, *Antechinus agilis*.
628 Mol. Ecol. 12, 475-484.

629 Leys, R., Watts, C.H.S. and Cooper, S.J.B. 2003. Evolution of subterranean diving beetles
630 (Coleoptera: Dytiscidae: Hydroporini, Bidessini) in the arid zone of Australia. *Evolution*, 57,
631 2819-2834.

632 Liedtke, H.C., Müller, H., Rödel, M.-O., Menegon, M., Gonwouo, N.L., Barej, M.F., Gvoždík,
633 V., Schmitz, A., Channing, A., Nagel, P. and Loader, S.P. 2016. No ecological opportunity
634 signal on a continental scale? Diversification and life-history evolution of African true toads
635 (Anura: Bufonidae). *Evolution*, 70, 1717-1733.

636 Losos, J.B. 2010. Adaptive radiation, ecological opportunity, and evolutionary determinism.
637 American Society of Naturalists E. O. Wilson award address. *Am. Nat.*, 175, 623-639.

638 Lv, X., Xia, L., Ge, D., Wu, Y. and Yang, Q. 2016. Climate niche conservatism and ecological
639 opportunity in the explosive radiation of arvicoline rodents (Arvicolinae, Cricetidae). *Evolution*,
640 70, 1094-1104.

641 Körtner, G. and Geiser, F. 2009. The key to winter survival: daily torpor in a small arid-zone
642 Marsupial. *Naturwissen.* 96, 525-530.

643 Krajewski, C., Woolley, P.A. and Westerman, M. 2000a. The evolution of reproductive
644 strategies in dasyurid marsupials: implications of molecular phylogenies. *Biol. J. Linn. Soc.*, 71,
645 417-435.

646 Krajewski, C., Wroe, S. and Westerman, M. 2000b. Molecular evidence for the pattern and
647 timing of cladogenesis in dasyurid marsupials. *Zool. J. Linn. Soc.* 130, 375-404.

648 Mahler, D.L., Revell, L.J., Glor, R.E. and Losos, J.B. 2010. Ecological opportunity and the rate
649 of morphological evolution in the diversification of Greater Antillean anoles. *Evolution*, 64,
650 2731-2745.

651 Maestri, R., Monteiro, L.R., Fornel, R., Upham, N.S., Patterson, B.D. and de Freitas, T.R.O.
652 2017. The ecology of a continental evolutionary radiation: Is the radiation of sigmodontine
653 rodents adaptive? *Evolution*, 71, 610-632.

654 Mayr, E. 1942. *Systematics and the origin of species*. Columbia Univ. Press, New York.

655 Mazel, F., Davies, J., Gallien, L., Renaud, J., Groussin, M., Münkemüller, t. and Thuiller, W.
656 2016. Influence of tree shape and evolutionary time-scale on phylogenetic diversity metrics.
657 *Ecography*, 39, 913-920.

658 Moen, D., Morlon, H. 2014. Why does diversification slow down? *Trends Ecol. Evol.*, 29, 190-
659 197.

660 Orme, D., Freckleton, R., Thomas, G., Petzoldt, T., Fritz, S., Isaac, N. and Pearse, W. 2012.
661 *caper*: comparative analyses of phylogenetics and evolution in R. Version 0.5.

662 Phillimore, A.B. and Price, T.D. 2008. Density-dependent cladogenesis in birds. *PLoS Biol.*, 6,
663 e71.

664 Pigot, A.L. Phillimore, A.B., Owens, I.P. and Orme, C.D. 2010. The shape and temporal
665 dynamics of phylogenetic trees arising from geographic speciation. *Syst. Biol.* 59: 660-673.

666 Pinto, G., Mahler, D.L., Harmon, L.J. and Losos, J.B. 2008. Testing the island effect in adaptive
667 radiation: rates and patterns of morphological diversification in Caribbean and mainland *Anolis*
668 lizards. *P. Roy. Soc. B Biol. Sci.*, 275, 2749-2757.

669 Porch, N. and Wyrwoll, K.-H. 2008. Birth of a biome: insights into the assembly and
670 maintenance of the Australian arid zone biota. *Mol. Ecol.*, 17, 4398-4417.

671 Price, S.L., Powell, S., Kronauer, D.J.C., Tran, L.A.P., Pierce, N.E. and Wayne, R.K. 2014.
672 Renewed diversification is associated with new ecological opportunity in the Neotropical turtle
673 ants. *J. Evolution. Biol.*, 27, 242-258.

674 Price, S.L., Etienne, R.S. and Powell, S. 2016. Tightly congruent bursts of lineage and
675 phenotypic diversification identified in a continental ant radiation. *Evolution*, 70, 903-912.

676 Pybus, O.G. and Harvey, P.H. 2000. Testing macro-evolutionary models using incomplete
677 molecular phylogenies. *Proc. R. Soc. Lond. B.*, 267, 2267-2272.

678 QGIS Development Team. 2016. QGIS Geographic Information System. Open Source
679 Geospatial Foundation. Available at: <http://qgis.osgeo.org>.

680 Rabosky, D.L. 2006. LASER: A Maximum Likelihood toolkit for detecting temporal shifts in
681 diversification rates from molecular phylogenies. *Evol. Bioinform.* 2, 247-250.

682 Rabosky, D.L. 2013. Diversity-dependence, ecological speciation, and the role of competition in
683 macroevolution. *Ann. Rev. Ecol. Evol. & Syst.* 44, 481-502.

684 Rabosky, D. L. and Lovette, I.J. 2008. Density dependent diversification in North American
685 wood-warblers. *Proc. R. Soc. Lond. B.*, 275, 2363-2371.

686 Rabosky, D.L., Donnellan, S.C., Talaba, A.L. and Lovette, I.J. 2007. Exceptional among-
687 lineage variation in diversification rates during the radiation of Australia's most diverse
688 vertebrate clade. *Proc. R. Soc. Lond. B: Biol. Sci.*, 274, 2915-2923.

689 Rabosky, D. L., Donnellan, S.C., Grundler, M. and Lovette, I.J. 2014. Analysis and
690 visualization of complex macroevolutionary dynamics: an example from Australian scincid
691 lizards. *Syst. Biol.*, 63, 610-627.

692 Rabosky, D. L., Grundler, M., Anderson, C., Title, P., Shi, J.J., Huang, H., Brown, J.W. and
693 Larson, J. 2017. BMMtools: an R package for the analysis of evolutionary dynamics on
694 phylogenetic trees. *Met. Ecol. Evol.*, 5, 701-707.

695 Revell, L.J. 2012. *phytools*: an R package for phylogenetic comparative biology (and other
696 things). *Met. Ecol. Evol.*, 3, 217-223.

697 Rodríguez, M.Á., López-Sañudo, I.L., Hawkins, B.A. 2006. The geographic distribution of
698 mammal body size in Europe. *Global Ecol. Biogeogr.*, 15, 173-181.

699 Schenk, J.J., Rowe, K.C. and Steppan, S.J. 2013. Ecological opportunity and incumbency in the
700 diversification of repeated continental colonizations by muroid rodents. *Syst. Biol.*, 62, 837-864.

701 Schluter, D. 2000. *The ecology of adaptive radiation*. Oxford Univ. Press, Oxford. 296 pp.

702 Schweizer, M., Hertwig, S.T. and Seehausen, O. 2014. Diversity versus disparity and the role of
703 ecological opportunity in a continental bird radiation. *J. Biogeogr.*, 41, 1301-1312.

704 Seehausen, O. 2006. African cichlid fish: a model system in adaptive radiation research. *Proc.*
705 *R. Soc. Lond. B*, 273, 1-12.

706 Simpson, G.G. 1944. *Tempo and mode in evolution*. Columbia Univ. Press, New York. 237 pp.

707 Simpson, G.G. 1953. *The major features of evolution*. Columbia Univ. Press, New York. 434
708 pp.

709 Slater, G.J. and Pennell, M.W. 2014. Robust regression and posterior predictive simulation
710 increase power to detect early bursts of trait evolution. *Syst. Biol.*, 63,293-308.

711 Slater, G. J. 2015a. Iterative adaptive radiations of fossil canids show no evidence for diversity-
712 dependent trait evolution. *Proc. Nat. Acad. Sci.*, 112, 4897-4902.

713 Slater, G. J. 2015b. Not-so-early bursts and the dynamic nature of morphological
714 diversification. *Proc. Nat. Acad. Sci.*, 112, 3595-3595

715 Stroud, J.T. and Losos, J.B. 2016. Ecological opportunity and adaptive radiation. *Ann. Rev.*
716 *Ecol. Evol. Syst.*, 47, 507-532.

717 Tran, L.A.P. 2014. The role of ecological opportunity in shaping disparate diversification
718 trajectories in a bicontinental primate radiation. *Proc. R. Soc. Lond. B*, 281, 20131979.

719 Van Dyck, S., Gynther, I. and Baker, A. 2013. *Field companion to the mammals of Australia*.
720 New Holland Publishers. 573 pp.

721 Venditti, C., Meade, A. and Pagel M. 2011. Multiple routes to mammalian diversity. *Nature*,
722 479, 393-396.

723 Weir, J.T. 2006. Divergent timing and patterns of species accumulation in lowland and highland
724 neotropical birds. *Evolution*, 60, 842-855.

725 Gohli, J. and Voje, K.L. 2016. An interspecific assessment of Bergmann's rule in 22
726 mammalian families. *BMC Evol. Biol.*, 16, 222.

727 Wagner, C.E., Harmon, L.J. and Seehausen, O. 2012. Ecological opportunity and sexual
728 selection together predict adaptive radiation. *Nature* 487, 366-369.

729 Webb, C.O., Ackerly, D.D., McPeck, M.A. and Donoghue, M.J. 2002. Phylogenies and
730 community ecology. *Ann. Rev. Ecol. Syst.*, 33, 475-505.

731 Westerman, M., Krajewski, C., Kear, B.P., Meehan, L., Meredith, R.W., Emerling, C.A. and
732 Springer, M.S. 2016. Phylogenetic relationships of dasyuromorphian marsupials revisited. *Zool.*
733 *J. Linn. Soc.* 176, 686-701.

734 Wroe, S. 2003. *Australian marsupial carnivores: recent advances in paleontology*. In: Jones,
735 M., Dickman, C. and Archer, M., eds. *Predators with pouches: the biology of carnivorous*
736 *marsupials*. Collingwood, Australia, CSIRO Publishing, 102-123.

737 Yoder, J.B., Clancey, E., Des Roches, S., Eastman, J.M., Gentry, L., Godsoe, W., Hagey, T.J.,
738 Jochimsen, D., Oswald, B.P., Robertson, J., Sarver, B.A.J., Schenk, J.J., Spear, S.F. and
739 Harmon, L.J. 2010. Ecological opportunity and the origin of adaptive radiations. *J. Evol. Biol.*,
740 23, 1581-1596.

741

742

743

744

745

746

747 *Figure captions*

748 **Figure 1** (a) Lineage-through-time (LTT) plot for dasyurids represented in form of log-
749 transformed lineage number (circles) and number of cumulative species (solid line). (b)
750 Disparity-through-time (DTT) plot for body mass. The solid line is the observed disparity and
751 the dashed line is the mean expected disparity derived from 10,000 simulations under Brownian
752 motion evolution. The grey area represents the 95% confidence interval. (c) Node height test
753 (NHT) plot showing absolute body mass (abs) contrasts against node height.

754

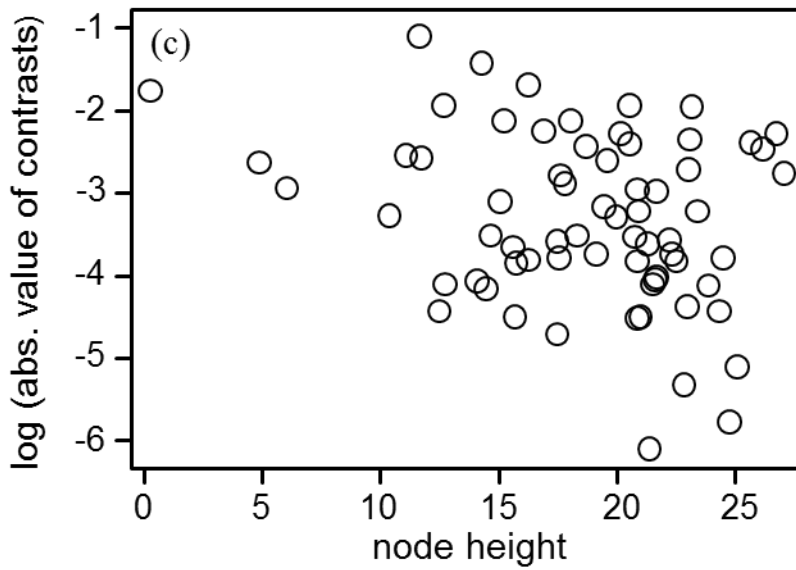
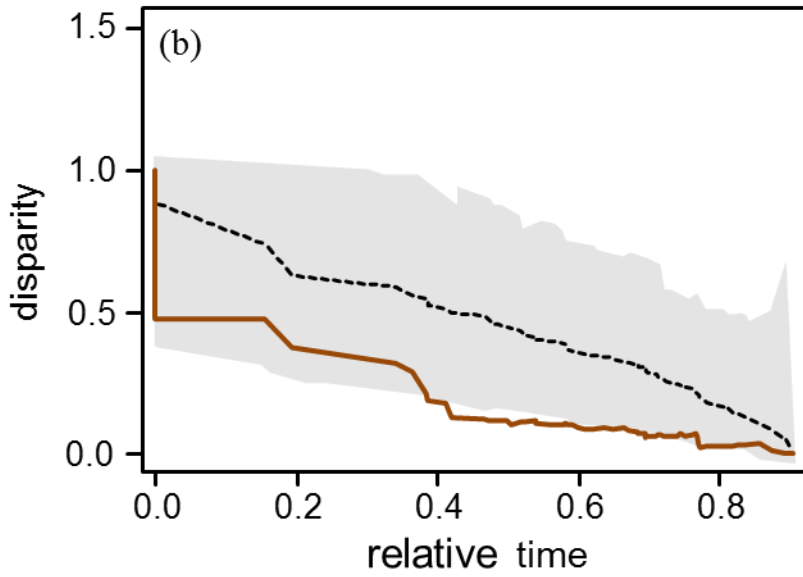
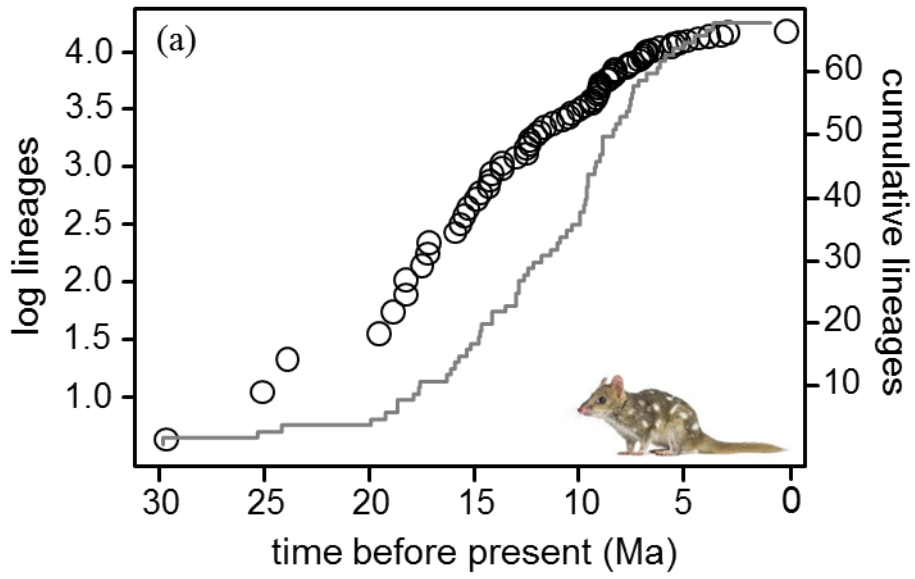
755 **Figure 2** The biogeographic regions inhabited by dasyurid species, mapped onto a Bayesian
756 phylogeny (MCC tree). Colour of the branches indicates the four different tribes. Colour coding
757 of the grid located at the right of the tips corresponds to the seven biogeographic regions
758 (orange: Eremaean; red: SW; purple: Bassian; pink: Tasmania; blue: Torresian; dark green:
759 Irian; light green: New Guinea). Photographs: Creative Commons and David Nelson.

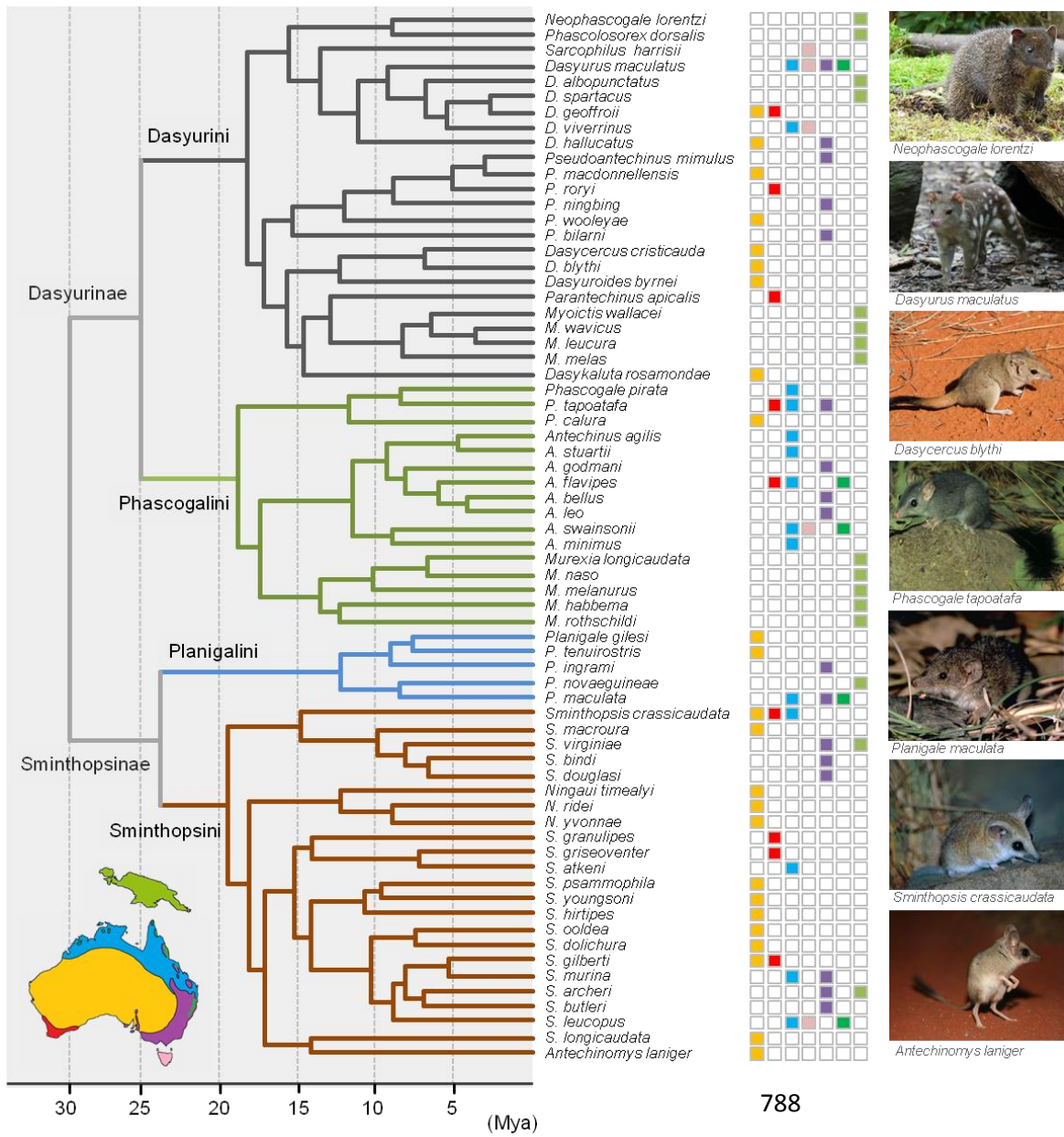
760

761 **Figure 3** Relationship between body mass and mean annual temperature in dasyurids
762 represented in the form of (a) standardized phylogenetic independent contrasts (PIC) and (b)
763 raw data.

764

765 Figure 1





789

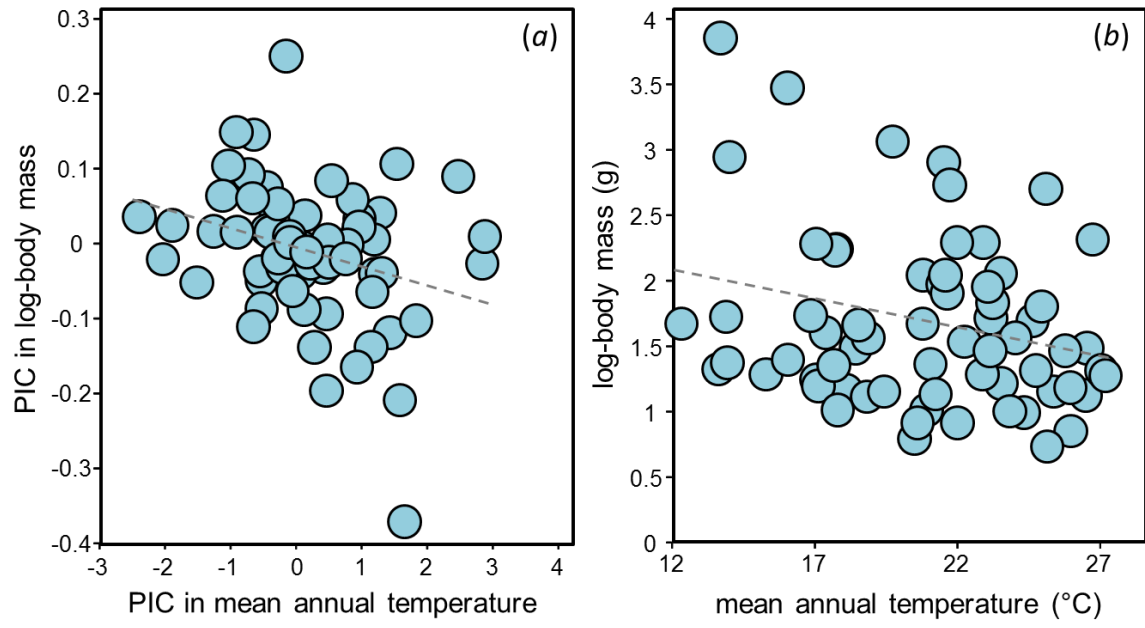
790

791 Figure 3

792

793

794



795 **Table 1** Results of the birth-death likelihood (BDL) analysis based on a) the Bayesian MCC
796 tree, and b) a set of 1000 trees randomly sampled from the posterior distribution of the MCMC
797 search. The following information is given: log-likelihood ($\ln L$), mean AIC value, difference in
798 mean AIC scores between each model and the overall best-fit model (Δ) and parameters (r = net
799 diversification rate in form of speciation events per million years; a = extinction fraction; k =
800 carrying capacity; x = magnitude of the rate change as a function of Nt) for each model (PB:
801 pure-birth model; BD: birth-death model; DDL: density-dependent logarithmic model; DDX:
802 density-dependent exponential model; yule2rate: Yule model with a shift).

	PB	BD	DDL	DDX	yule2rate²
b) MCC tree					
Parameters	$r_1 = 0.084$	$r_1 = 0.084$ $a = 0$	$r_1 = 0.298$ $k^1 = 69.930$	$r_1 = 0.548$ $x^1 = 0.526$	$r_1 = 0.120$ $r_2 = 0.008$ $t = 3.710$
$\ln(L)$	-11.344	-11.344	12.586	-2.613	12.043
ΔAIC	45.860	47.860	0	30.397	3.085
a) 1000 trees					
Parameters	$r_1 = 0.089$	$r_1 = 0.089$ $a = 0$	$r_1 = 0.310$ $k^1 = 70.118$	$r_1 = 0.592$ $x^1 = 0.532$	$r_1 = 0.123$ $r_2 = 0.009$ $t = 3.227$
$\ln(L)$	-7.494	-7.494	15.634	1.255	16.037
ΔAIC	44.256	46.256	0	28.757	1.194

803 ¹ More complex variants of the Yule model, that is, models assuming constant speciation rates within
804 more than two intervals (Yule3rate, Yule4rate, Yule5rate) did not provide a better fit (lower AICc
805 values) than the best model (DDL) and therefore, these are not reported.

806

807 **Table 2** Relative fit of three alternative models (“niche-filling” or early-burst, EB; Ornstein-
 808 Uhlenbeck, OU; Brownian motion, BM) to body mass of Dasyurinae. Values obtained from the
 809 MCC tree and values summarized across 1000 chronograms randomly sampled from the
 810 posterior distribution of the BEAST MCMC analysis are shown.

811

812

813

	EB	OU	BM
(a) MCC tree			
$\ln(L)$	-17.887	-22.812	-22.812
ΔAIC_c	0	9.849	7.658
AIC_w	0.971	0.007	0.021
(b) 1000 trees			
$\ln(L)$	-18.475	-22.405	-22.405
ΔAIC_c	0	7.859	5.669
AIC_w	0.873	0.036	0.089

814 **Table 3** Community phylogenetic results for the seven biogeographic regions. *N* is the number
815 of taxa occurring in each region. Observed values, randomized values (null model), *z*-values for
816 the observed value based on the randomization tests and *p*-values were calculated for both
817 measures: mean pairwise distance (MPD) and mean nearest taxon distance (MNTD). Significant
818 values are indicated in bold.

819

	<i>N</i>	Observed	Random.	<i>z</i> -value	<i>p</i> -value
(a) MPD					
Eremaean	24	45.81	47.23	-2.46	0.029
SW	9	45.28	43.85	0.87	0.821
NTE	14	44.52	45.79	-1.19	0.114
Tasmania	5	36.77	39.54	-0.94	0.157
Torresian	17	46.87	46.38	0.56	0.684
Irian	5	42.06	39.57	0.88	0.823
New Guinea	16	43.01	46.20	-3.33	0.008
(b) MNTD					
Eremaean	24	22.71	22.29	0.27	0.617
SW	9	33.99	29.35	1.30	0.914
NTE	14	21.23	25.80	-1.81	0.044
Tasmania	5	34.69	35.99	-0.18	0.405
Torresian	17	18.72	24.32	-2.68	0.006
Irian	5	38.30	35.83	0.44	0.608
New Guinea	16	20.63	24.86	-1.92	0.036

820

821

822

823

824

825

826

827

828